

## STUDY ON STRENGTHENING METHOD FOR EXISTING CONCRETE STRUCTURES USING TENSIONED CFRP PLATE

(Translation from Proceedings of JSCE, No.711/V-56, August 2002)



Yuzuru HAMADA



Masumi INOUE



Akira KOBAYASHI



Nobuaki TAKAGI



Takayuki KOJIMA

This paper presents the results of static and fatigue tests of RC beams strengthened with non-tensioned and tensioned CFRP. This plate was fabricated by Pultrusion method with carbon fiber, which has a guaranteed tensile capacity of 234kN and elastic modulus of 150 kN/mm<sup>2</sup>. From this investigation, it is evident that CFRP plates can increase the flexural capacity of RC beams. Tensioned CFRP plates are more effective at strengthening than unstressed plates. This was further enhanced by arranging an intermediate anchoring device. It is also evident that CFRP plates can increase the fatigue strength of RC beams.

**Keywords** : CFRP plate, flexural strengthening, peeling, fatigue test

---

Yuzuru Hamada is a manager in Research and Development Center at DPS Bridge Works Co.,Ltd., Tokyo. He received his Doctor of Engineering Degree from Ritsumeikan University in 2002. His research interests relate to the durability and maintenance of prestressed concrete structures. He is a member of JPCEA, JCI and JSCE.

Masumi Inoue is a postdoctoral fellow in the Organization for the Promotion of the COE Program at Ritsumeikan University. He received his Doctor of Engineering Degree from Ritsumeikan University in 2003. His research interest includes concrete structure member using continuous fiber reinforcement. He is a member of JSCE.

Akira Kobayashi is a general manager in the technical developing department at Nippon steel composite Co. ltd. He is a member of Japan Concrete Institute technical committee on retrofit technology for concrete structures. He is a member of JSCE and JCI.

Nobuaki Takagi is a professor in the Department of Civil Engineering at Ritsumeikan University, Japan. He received his Doctor of Engineering Degree from the Kyoto University in 1994. He specializes in silica fume concrete and concrete member using new fiber material. He is a member of JSCE.

Takayuki Kojima is a professor in the Department of Civil Engineering at Ritsumeikan University, Japan. He received his Doctor of Engineering Degree from the Kyoto University in 1983. He specializes in finite element analysis of crack propagation of concrete member and concrete member using new fiber material and torsion of concrete member. He is a member of JSCE.

---

## **1. INTRODUCTION**

With increased concern about the life cycle of the existing infra structure, there is an urgent need to establish maintenance systems for concrete structures. The most important maintenance that can be applied to existing structures is strengthening as a way to recover and improve the load-bearing capacity [1]. However, no proper guidelines for the selection and design of strengthening methods have yet been established. This is simply because of the huge variety of structural types and combinations of strengthening methods. Consequently, there is a need for proper recommendations or manuals in which the effectiveness and the applicability of strengthening methods so far proposed and used are assessed.

Conventional strengthening methods for reinforced concrete (RC) members, which include the steel-plate bonding method and the steel-plate or RC jacketing method, have been widely applied. These methods excel in cost performance, because conventional materials such as steel plate, steel bar and concrete are used. And if adequate bonding between reinforcing materials and existing concrete member is assured, the design of the strengthening procedure can be made use of methods similar to those for normal usual RC design. However, there will always be some situations in which these methods are not applicable because of the problem such as the higher dead load, the durability in a corrosive environment, or the workability under tight space limitations.

On the other hand, continuous fiber sheet is an excellent strengthening material with good strength, stiffness, and corrosion resistance. It is much lighter and more flexible than steel. A highly workable strengthening method is to bond continuous fiber sheet to the outside of an existing concrete structure or wrap it around the structure by using epoxy resin. Since the Kobe Earthquake of 1995, the strengthening of existing RC columns against shear and ductility has become a matter of particular urgency, and many investigations on the strengthening effect of continuous fiber sheet have been carried out. Recently, results related to the strengthening of RC slabs and RC beams have also been accumulated, and design and construction guidelines for the repair and strengthening of concrete road bridges using the carbon fiber sheet bonding method [2] are being prepared. The strengthening effects of these methods only improve the live load capacity, however, since the continuous fiber sheeting or steel plates are generally bonded to the existing structure while it is under the dead load. Consequently, this method does not contribute to functionality at the serviceability limit state, such as by reducing the stress on the reinforcement or reducing the width of existing cracks under the dead load. Further, it has been indicated that the flexural capacity of RC beam strengthened using the continuous fiber sheet bonding method must be calculated in consideration of the possibility of peeling of the fiber sheet [3], and that present strengthening techniques do not take full advantage of the high strength of continuous fiber sheet.

In this study, the authors examined the strengthening effects of tensioned carbon fiber reinforced polymer plate (CFRP plate) when applied to concrete structures and examined how to estimate the resulting ultimate load, with the aim of bringing this method into practical use. By tensioning a CFRP plate and then anchoring it under tension to the concrete member, it was possible to take full advantage of the high strength of CFRP. The introduction of prestress improved stress conditions and reduced deformation under the dead load or excessive loading, thus controlling crack width. Furthermore, the ultimate load capacity of a beam strengthened with a tensioned CFRP plate notably increased.

In the field of the bridge maintenance, the post-tensioned external tendons are often used for strengthening [4]. Large amounts of cable are usually required for this method [5], and anchoring members, such as an additional cross beam or concrete block, must be provided in many cases. Further, this method generally finds application where the bridge is large, such as for post-tensioned T-beam bridges and box girder bridges, because there must be adequate space to fit external cables and anchorages. In strengthening with tensioned CFRP plate, the device used to tension the CFRP plate is directly attached to the concrete member and the CFRP plate is bonded to the concrete. This makes it comparatively easy to carry out strengthening work, since no special anchoring member needs to be installed. Also, no space needs to be reserved for installation of tendons; instead, the finished surface after bonding is flat. However, the tensile capacity of the CFRP plate is lower than that of tendon consisting of external cable, because it is difficult to introduce uniform tension force over the width of the plate, particularly when the plate is increased in width to obtain greater tensile capacity. For these reasons, the strengthening method proposed in this study is thought to be most suitable for the flexural strengthening of slabs or hollow slab road bridges of comparatively small scale.

The dimensions of the CFRP plates used here are 50mm (width) × 2mm (thickness). The tensile strength of a plate and the characteristics of the tensioning device were examined through direct tensile tests. Static tests of RC beams strengthened using tensioned CFRP plates were carried out under flexural loading, so as to investigate the effects of

plate tension on the load-bearing capacity and the deformability of the beams. Further, fatigue tests were carried out to investigate the fatigue performance and fatigue strength of the strengthened beams. The strengthening procedure, begins with tensioning the CFRP plate in a convenient steel frame using conventional post-tensioning jacks. Epoxy resin is then spread over the plate, and the tensioning devices are fixed to the concrete member using high-tension bolts and connectors prepared in advance on the underside of the beam. In some cases, intermediate anchoring plates are also attached to each shear span using high-tension bolts and similar embedded connectors. At this point, the tensioning frame can be released.

## 2. TENSILE TESTING OF CFRP PLATES

### 2.1 Outline of experiment

In order to confirm the tensile strength of the CFRP plate and the characteristics of the tensioning devices, tensile tests were carried out prior to the loading tests on actual beams. The properties and specifications of the two raw materials (carbon fiber sheet and resin) and the composite CFRP plate are given in **Table 1**. The tensile capacity and modulus of elasticity of the CFRP plate are theoretical values based on the assumption that bonding between carbon fiber and epoxy resin is complete [6].

**Table 1** Properties and specifications of composite materials

Carbon fiber		
Modulus of elasticity	(kN/mm <sup>2</sup> )	235
Tensile strength	(N/mm <sup>2</sup> )	4850
Resin		
Modulus of elasticity	(kN/mm <sup>2</sup> )	2.94
Tensile strength	(N/mm <sup>2</sup> )	75
Specifications of carbon fiber plate (theoretical values)		
Width	(mm)	50
Thickness	(mm)	2
Fiber volume ratio	(%)	62.2
Modulus of elasticity	(kN/mm <sup>2</sup> )	148
Tensile strength	(N/mm <sup>2</sup> )	3050

The plates were fabricated from high-tensile-strength carbon fiber using the Pultrusion method. The fiber volume ratio of the plates is 62.2%. The tensioning device consists of a steel sleeve (external diameter: 76.3 mm; thickness: 9.5 mm; STPG375; yield strength: 216 N/mm<sup>2</sup>). One tensioning device is pushed over each end of the CFRP plate, and expansive paste with a nominal expansive pressure of 30 N/mm<sup>2</sup> was poured into the sleeve around the plate. The expansive pressure of the paste anchors the plates into the sleeves [7]. For the tensile tests, the specimens were cured at 20 degrees and RH 90% for about one week.

A tensile test specimen is shown in **Fig. 1**. The test length of CFRP plate was 500 mm, corresponding to ten times

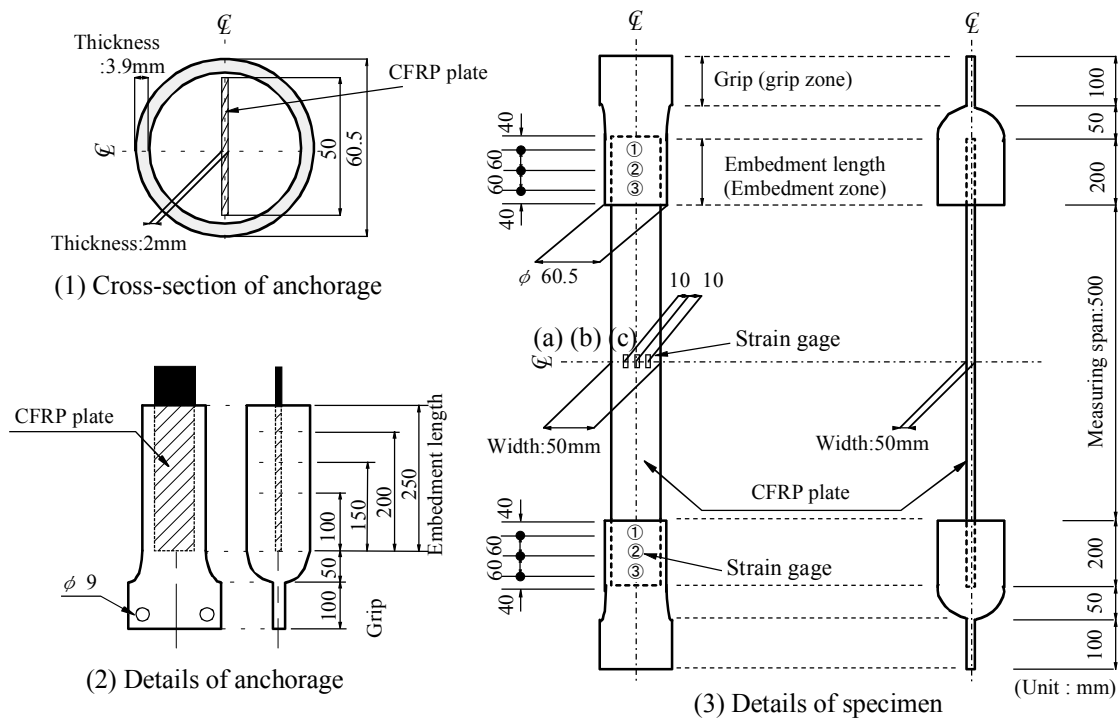


**Fig. 1** Specimen for tensile test

the width of the plate. In order to reduce the weight added to the structure by continuous fiber reinforcement, it is necessary to make the tensioning device as light as possible. Four different lengths of steel sleeve (100, 150, 200, and 250 mm) were chosen for testing, and the effect of embedment length on anchoring properties was examined.

In the direct tensile tests, specimens were carefully placed in the grips of a testing machine to ensure that there was no eccentric force. In cases where the grip zones of the specimen had become misshapen as a result of expansive material pressure, the grips were placed on the actual anchor(embedment) zones of the steel sleeves. The maximum load and strains at the center of the plate were measured, and failure conditions confirmed. In order to confirm the pressure exerted by the expansive material, the change in strain of steel sleeve was measured from casting of the expansive material until tensile testing.

## 2.2 Results and discussions

The results of the tensile tests on CFRP plates are shown in **Table 2**. Regarding the average maximum plate load for each anchorage embedment length, the ratio to a theoretical value calculated from theoretical strength (**Table 1**) is also shown. In all specimens with 100, 150, and 200 mm embedment length, slip failure occurred in the anchorage of the tensioning device. For all specimens with a 250 mm embedment length, failure consisted of rupture of the plate; no slip failure was observed even in the ultimate state. (Some specimens with a 250 mm embedment length were gripped directly by the embedment zone at one or both ends for the tests.)

The relationship between embedment length and maximum plate load is shown in **Fig. 2**. There is an approximately linear relationship in specimens where slip failure was observed in the anchorage. The least-squares regression line for these specimens (that is, the specimens with 100, 150, and 200 mm embedment length) is shown extended up to the range of 250 mm embedment length. The maximum load for specimens with a 250 mm embedment length falls

**Table 2** Results of tensile tests

Specimen	Embedment length (mm)	Maximum load (kN)	Failure pattern
C10-1	100	136	S
C10-2		129	S
Average		132 (43%)	
C15-1	150	204	S
C15-2		182	S
Average		193 (63%)	
C20-1	200	254	S
C20-2		216	S
Average		235 (77%)	
C25-1 #	250	245	F
C25-2 #		269	F
C25-3 #		265	F
C25-4 #		252	F
C25-5 #		250	F
C25-6 #		266	F
C25-7 #		252	F
C25-8 #		261	F
C25-9 #		254	F
C25-10		259	F
Average	257 (84%)		

#: Directly gripping embedment zone of steel sleeve  
 Failure pattern S : Slipping of plate, F : Failure of plate  
 ( ): Maximum load/theoretical value (=305kN)

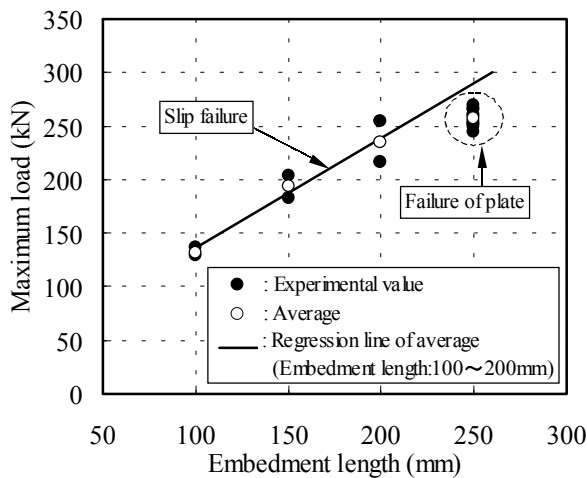


**Fig. 2** Relationship between embedment length and maximum plate load

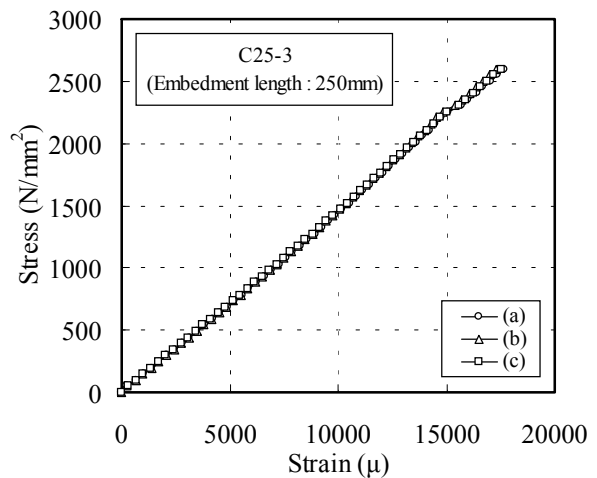


**Fig. 3** Relationship between plate stress and strain

below the regression line in every case. This results from the change in failure mode. In the specimens with a 250 mm embedment length, the variation in maximum load is relatively small, and there is no notable difference between specimens gripped normally and those gripped at the embedment zone. This demonstrates that, with a 250 mm embedment length, the failure mode is rupture of the plate regardless of the grip method; consequently, the high strength of the CFRP plate can be used effectively. The average maximum load of specimens with a 250 mm embedment length was 257 kN. The coefficient of variation was 3.07%, and the tensile strength calculated by the 3  $\sigma$  method was 234kN.

The stress-strain relationship of the plate is shown in **Fig. 3**. The experimental values of strains measured at three points near the center of the plate are also shown. All values are similar, so it can be inferred that the tensile force was uniformly distributed over the width of the plate. The stress-strain relationship is linear up to failure. In the specimens with a 250 mm embedment length, the average modulus of elasticity calculated using 20% and 60% of the maximum load was 150 kN/mm<sup>2</sup>, which was approximately equal to the theoretical value (**Table 1**).

### **3. RC BEAM SPECIMENS AND STRENGTHENING METHOD**

#### **3.1 Materials**

The dimensions and tensile test results for CFRP plates used are shown in **Table 3**. Epoxy resin was used to bond CFRP plate to RC beam.

The mix proportion of concrete is shown in **Table 4**. Normal Portland cement (specific gravity: 3.16 g/cm<sup>3</sup>) was used, and the water-cement ratio was 52%. The mechanical properties of the concrete at the introduction of flexural crack to RC beams and at the loading tests are shown in **Table 5**.

**Table 3** Mechanical properties of CFRP plate

Width	(mm)	50
Depth	(mm)	2
Tensile capacity	(kN)	234
Modulus of elasticity	(kN/mm <sup>2</sup> )	150
Maximum strain	( $\mu$ )	15600

**Table 5** Mechanical properties of concrete (N/mm<sup>2</sup>)

	at introduction of flexural crack	at loading test
Compressive strength	29.5	38.9
Tensile strength	2.72	2.96
Modulus of rupture	5.41	6.94
Modulus of elasticity	32000	32000

**Table 4** Mix proportion of concrete

W/C (%)	s/a (%)	Unit content (kg/m <sup>3</sup> )							Slump (cm)	Air content (%)
		W	C	S	G1	G2	G3	Ad		
52	41.9	157	302	756	215	323	539	0.755	8.3	4.7

S.G. : Specific gravity

#### **3.2 RC beam specimens**

RC beam specimen is shown in **Fig. 4**. The size of beam is 400 x 200 x 3,000 mm. Deformed bars with a diameter of 16mm (SD295; yield strength: 355 N/mm<sup>2</sup>; tensile strength: 517 N/mm<sup>2</sup>) were used for longitudinal reinforcement. The effective depth was 154 mm, and the longitudinal reinforcement ratio was 1.29%. Deformed bars with a diameter of 13mm (SD295; yield strength: 368 N/mm<sup>2</sup>; tensile strength: 528 N/mm<sup>2</sup>) were used at 100 mm spacing in the shear spans as stirrups to ensure that shear failure would not occur before flexural failure. The shear reinforcement ratio was 0.63%. To allow for attachment of the tensioned CFRP plate, a notch (90 x 40 x 270 mm) was prepared on the bottom surface of the beam near each support bearing point.

#### **3.3 Strengthening method**

Based on the tensile test results of CFRP plates, a tensioning device with 250 mm long was chosen, as shown in **Fig. 5**. A steel sleeve (external diameter: 76.3 mm; thickness: 9.5 mm) was used as the anchorage, and a steel plate was welded to the sleeve for later attachment to the beam. Expansive paste with a nominal expansive pressure of 30 N/mm<sup>2</sup> was poured into sleeve to form the anchorage. The welding length of the anchor plate, and the specifications

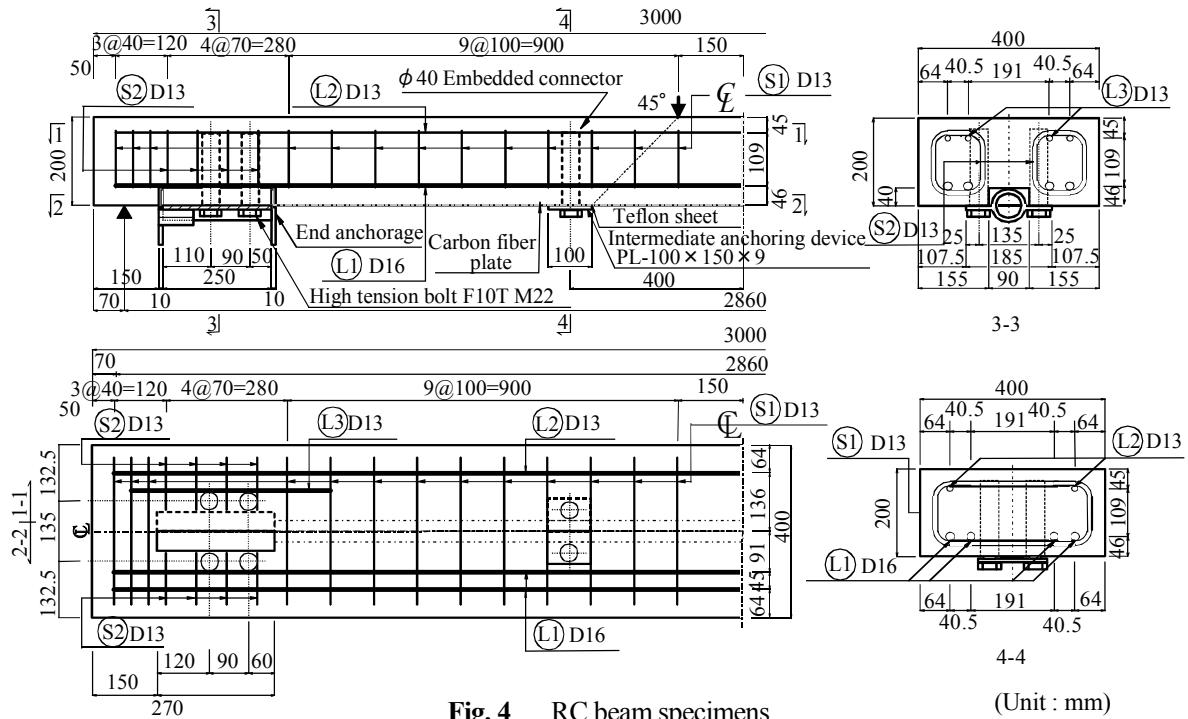


Fig. 4 RC beam specimens

(Unit : mm)

and the number of embedded anchors were decided based on the tensile strength of the plate.

The CFRP plate was tensioned using the procedure shown in Fig. 6. Prestress would generally be introduced by tensioning the anchorages using a special post-tensioning system. However, in the case of small RC beams, such the specimens used here, the application of prestress using a steel frame as shown in Fig. 6 is convenient. In this study, therefore, prestress was introduced using a convenient frame constructed with hot-rolled steel components.

First, the plate was cut to the designed length, and tensioning devices were anchored to the ends of the plate using expansive paste, as already described. The anchorages were left to cure for about a week. Where

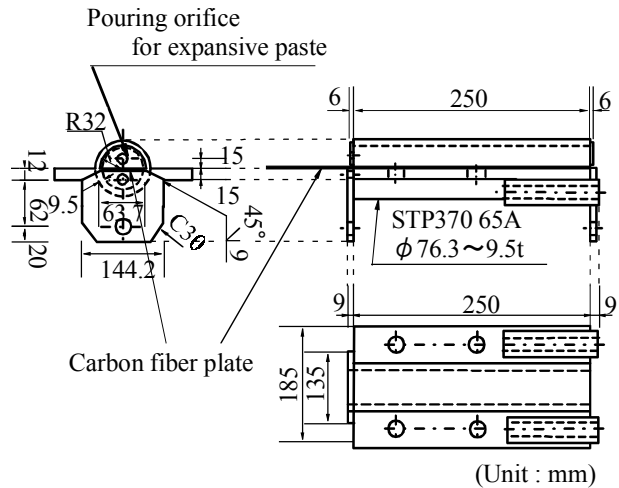


Fig. 5 Details of end anchorage

(Unit : mm)

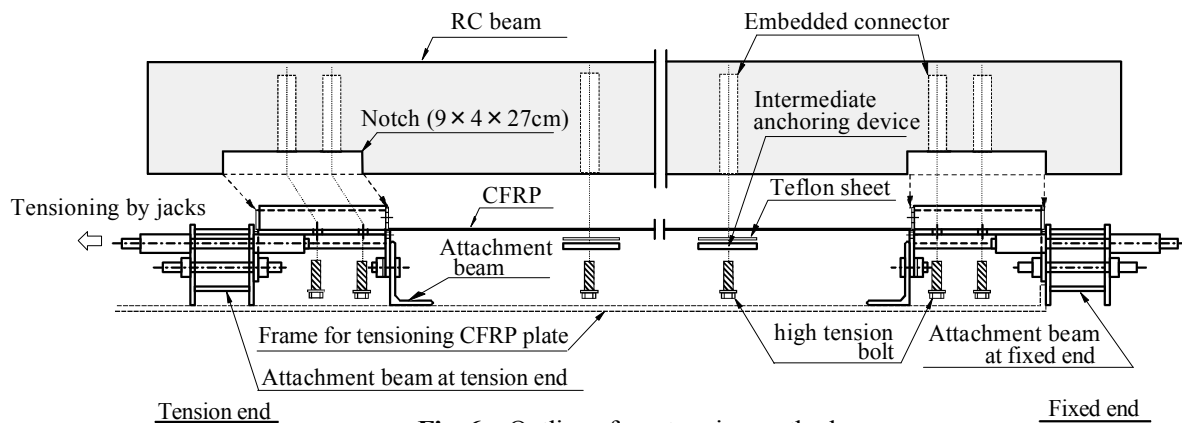


Fig. 6 Outline of prestressing method

the plate was to be bonded to the RC beam surface, the area was roughened using a disc-sander, and the roughened surface was treated with a primer. After the curing of the primer, the plate was tensioned and anchored to the steel frame by using conventional post-tensioning jacks. The plate was coated with epoxy resin, and the two tensioning devices were attached to the beam using high-tension bolts (F10T; M22 mm) at the embedded connectors. Finally, the frame tension was released, leaving the plate bonded to the concrete surface.

With this strengthening method, there is a possibility of peeling failure in the vicinity of flexural shear cracks, since the plate is thicker than the continuous fiber sheet itself. To prevent this, intermediate anchoring plates (100 x 150 x 9 mm) were also attached in each shear span with high-tension bolts before the epoxy resin hardened. Similarly, embedded connectors were fitted to some beams in order to restrain and delay peeling of the plate. A sheet of Teflon was inserted between the plate and the intermediate anchoring plates in order to prevent corner-failure of the plate. The installation of an intermediate anchoring device is illustrated in Fig. 7.

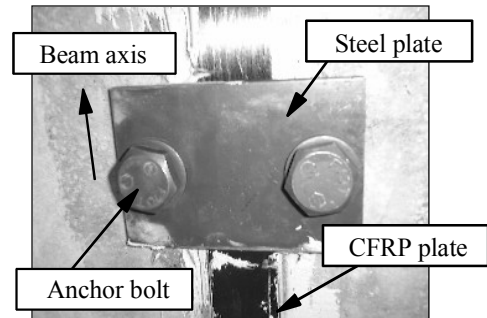


Fig. 7 Intermediate anchoring device

This strengthening method has the advantage that the prestress was mechanically maintained by attaching the tensioning device to the beam. On the contrary, conventional strengthening methods rely on externally introduced prestress that is removed once the epoxy resin hardens [8]. So one advantage of this new strengthening method is that equipment required for the tensioning work can be removed immediately. The method also avoids the known problem of peeling of the sheet ends at relatively high levels of tensioning force when using conventional methods based on continuous fiber reinforced sheet [9].

Similar problems might be expected when using FRP plates, but the tensioning device used here also functions to prevent peeling at the end of the plate. On the contrary, in case of saving the construction labor, it is also thought that the plate was used without bonding to the concrete surface like external cable method. But the assumption of “plane sections remain plane” can not be applied for the beam strengthening by the un-bonded plate, and its flexural capacity decreases because the amount of the stress increase in the plate decreases. On the other hand, in this strengthening method of bonding between plate and concrete, the assumption of “plane sections remain plane” can apply until the peeling of the plate occurs. As a result, the amount of the stress increase in the plate increases in comparison with the case of un-bonded plate. It is also thought that the flexural capacity of strengthened RC beams is improved by restrained and delayed peeling of the plate resulting from use of the intermediate anchoring device.

### 3.4 Loading conditions and measurements

Test loading conditions and measurements are illustrated in Fig. 8. Specimens used for static and fatigue loading

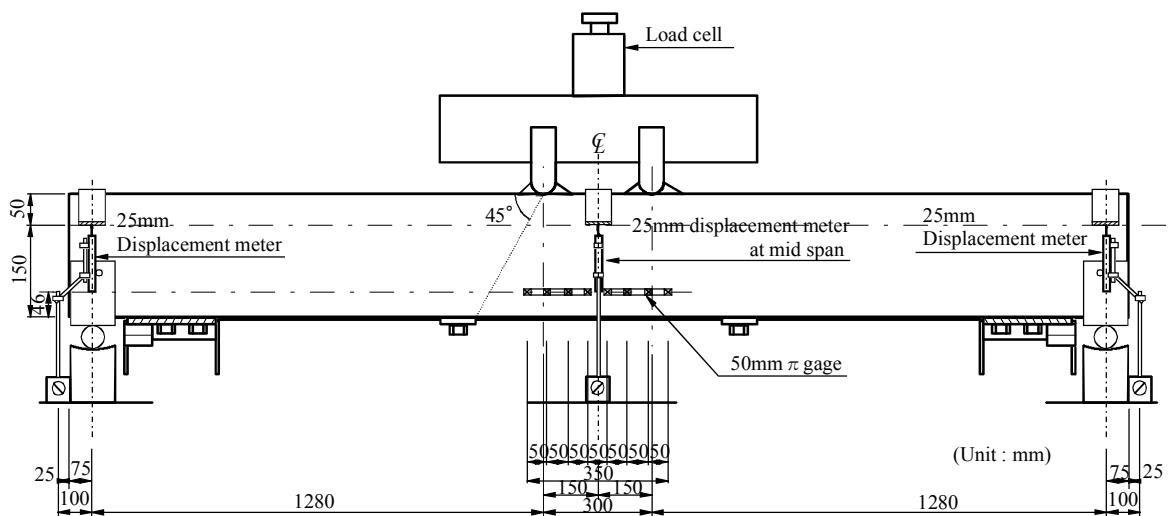


Fig. 8 Loading conditions and measurements

tests had a span of 2,860 mm and a flexural span of 300 mm. The shear span effective depth ratio ( $a/d$ ) was a constant 8.31. Concrete strain at the compressive fiber in the center of the span, the longitudinal reinforcement and plate strains, and the deflection and crack width at mid-span, were measured. Longitudinal reinforcement and plate strains were measured both at mid span and also at one location in each shear span. Plate strains were measured continuously from before prestressing until the end of loading.

#### 4. STATIC LOADING TEST OF STRENGTHENED RC BEAMS

##### 4.1 Outline of experiment

A summary of the static loading tests is given in **Table 6**. Sound RC beams (Type N), and deteriorated RC beams (Type D) that had been loaded up to yielding of the longitudinal reinforcement prior to strengthening were used. The tension applied to the plates was 0%, 25% and 50% of the tensile strength of the plate itself. In the case of zero tension (N-00 specimen), it is thought that sag occurred as a result of anchoring a non-tensioned plate, so in fact the plate tension in the N-00 specimen was 5%. In some beams, intermediate anchoring devices were attached in the shear span.

**Table 6** Summary of static loading tests

Specimen	Introduction of crack before strengthening	Tensile force of plate (kN)	Intermediate anchoring device
N	Reference beam		
N-00	None (Sound beam)	11.4 [5%]	Not used
N-25P		58.2 [25%]	Used
N-50		116.8 [50%]	Not used
N-50P		116.8 [50%]	Used
D-25P	Introduced (Deteriorated beam)	58.2 [25%]	Used
D-50		116.8 [50%]	Not used
D-50P		116.8 [50%]	Used

[ ] : Tensile force/tensile strength of plate

##### 4.2 Loading method

The loading conditions are shown in **Fig. 8**. The load was relaxed after the initial occurrence of flexural cracking, and then the load was monotonously increased until failure of the beam.

##### 4.3 Test results and discussions

The results of the static loading test are shown in **Table 7**. All specimens strengthened using the tensioned plate failed in flexure immediately the following peeling of the plate, and no plate failure was observed even in the ultimate state. The end tensioning devices and intermediate anchorages remained sound, as did the concrete around them; no deterioration was observed even at failure of the beam.

**Table 7** Results of static loading test

Specimen	$\eta$ (%)	$P_{cr}$	$P_y$	$P_{stp}$	$P_{u,exp}$	$P_{u,cal}$			
						Perfect bond*	A method	B method	C method
N		11	58	---	67	61 [1.10]	—	—	—
N-00	1	18	72	86	86	114 [0.75]	66 [1.30]	83 [1.04]	85 [1.02]
N-25P	10	10	81	109	110	117 [0.94]	72 [1.53]	99 [1.11]	100 [1.10]
N-50	38	39	100	110	113	129 [0.88]	90 [1.26]	106 [1.07]	108 [1.05]
N-50P	34	34	106	126	126	127 [0.99]	87 [1.45]	114 [1.10]	115 [1.10]
D-25P	26	{10}	86 (58)	110	110	124 [0.89]	82 [1.34]	109 [1.01]	110 [1.00]
D-50	31	{7}	89 (58)	104	104	126 [0.82]	85 [1.23]	101 [1.03]	103 [1.01]
D-50P	48	{5}	106 (60)	126	126	133 [0.95]	96 [1.32]	122 [1.03]	123 [1.02]

$P_{cr}$  : Flexural cracking load,  $P_y$  : Yield load,  $P_{stp}$  : Peeling load of plate

$P_{u,exp}$  : Experimental value of ultimate load,  $P_{u,cal}$  : Calculated value of ultimate load

$\eta$  : Measured tensile force/tensile strength of plate

Perfect bond\* : Calculated value of ultimate load on assumption that plane sections remain plane

{ } : Initial flexural cracking load before strengthening

( ) : Maximum load applied to introduce flexural crack before strengthening, [ ] :  $P_{u,exp}/P_{u,cal}$

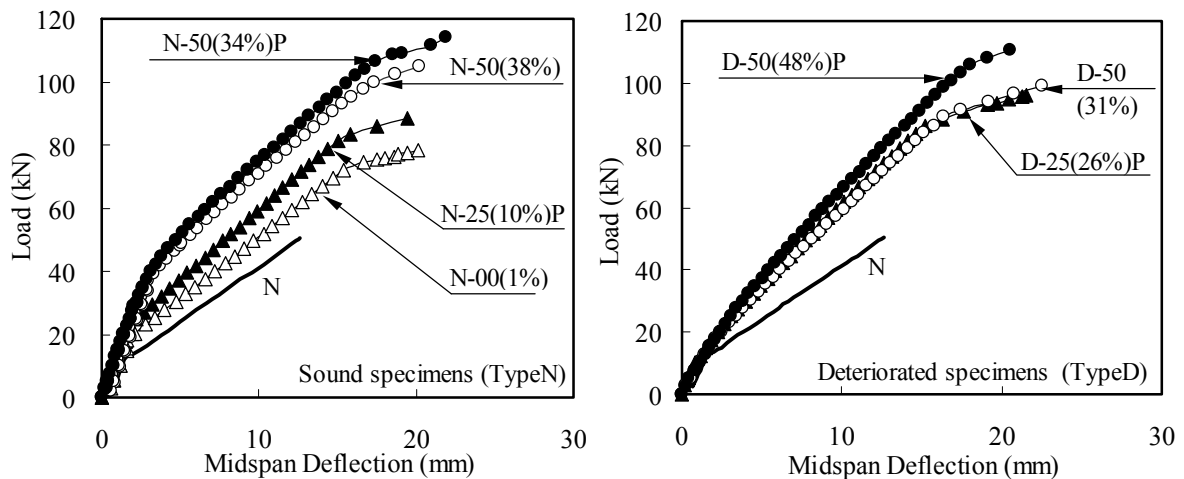


Fig. 9 Relationship between load and deflection at mid span

a) Effective tension of plate

The ratios of effective tensile force and tensile capacity of the plate are shown in Table 7. Effective tensile forces were calculated by multiplying the plate strain before the loading by the modulus of elasticity and sectional area of the plate. In specimens D-25P and D-50P, it was possible to introduce the target plate tensile force. However, the target value could not be achieved in other specimens as a result of placement errors in the embedded connectors and production errors in the end tensioning device. It will be necessary to develop a tensioning and anchorage system by which the plate can be tensioned with accuracy, and which can be made the adjustment of tensile force relatively easy.

b) Deflection

The relationship between load and deflection at mid span is shown in Fig. 9. In the case of the deteriorated beams (Type D specimen), the deflection is the value upon reloading after strengthening. The flexural cracking load in the sound beams (Type N specimen) increased with rising plate tensile force. The yield load increased linearly with plate tensile force, no matter how much the beam had deteriorated. In comparison with the deflection curves for specimen N-50 and specimen N-50P, the yield load and flexural stiffness (EI) of the cross section tended to be higher if intermediate anchoring devices were installed. That is, the installation of intermediate anchoring devices was an effective way to improve the load-bearing capacity and deformability of the beam.

The relationship between load and crack width for strengthened RC beams (effective tensile force: 50%) and the reference beam without strengthening (Type N specimen) is shown in Fig. 10. The crack width in the deteriorated beams (Type D specimen) is the value during reloading after strengthening. The residual crack width of deteriorated beams was about 0.1 mm after initial loading. It is confirmed that the residual crack width after strengthening is much lower, and is too small to be determined by visual observations. No new cracks occurred upon reloading after strengthening in the case of deteriorated beams, and crack width increased linearly on reloading. As a result, the crack width of the deteriorated beam was a little greater than that of the sound beam for any given tensile force. Similarly, the deflection of the deteriorated beam was somewhat greater than that of the sound beam, as shown in Fig. 9. However, it was clarified that cracks were narrower in strengthened RC beams than in

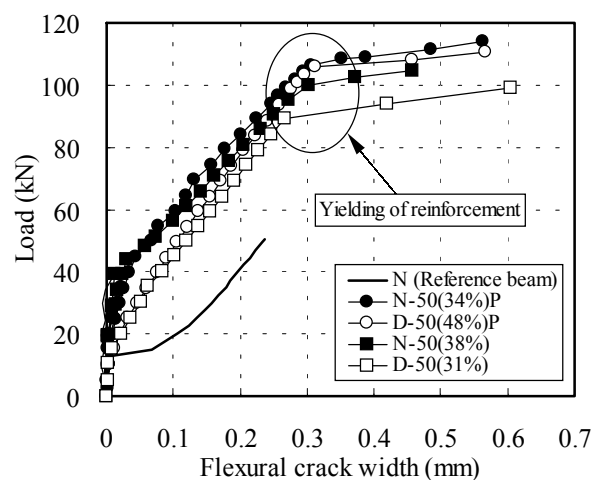


Fig. 10 Relationship between load and flexural crack width

unstrengthened beams, regardless of the prior deteriorated state, and the width of flexural cracks in deteriorated beams was controlled after strengthening with tensioned CFRP plates.

c) Longitudinal reinforcement and plate strains

The relationships between load and strains for the longitudinal reinforcement and the plate are shown in Fig. 11. In the case of sound beams, plate strain increased linearly after initial occurrence of flexural cracking until yielding of the longitudinal reinforcement. In the case of deteriorated beams, longitudinal reinforcement strain and plate strains increased linearly from the start of loading until yielding of the longitudinal reinforcement. Also, beyond the yielding of the longitudinal reinforcement, plate strain increased at a rapid and constant rate in both sound and deteriorated beams until beam failure. It is thought that the peeling observed near flexural cracks before failure was partial only. This suggests that adequate bonding between plate and concrete is achieved, and the CFRP plate effectively carries load even after the yielding point of longitudinal reinforcement. The ratio of total strain at mid span to maximum plate strain is shown in Fig. 12. (The maximum strain is the strain corresponding to the tensile capacity of the plate.) The total plate strain at mid span reached at least 70% of the maximum strain, regardless of use of the intermediate anchoring device, when the effective tensile force of the plate was more than 25% of tensile capacity. Furthermore, the total plate strain reached 83%-97% of maximum strain when the intermediate anchoring device was used. This confirms that the tensile capacity of the plate is effectively used in this application.

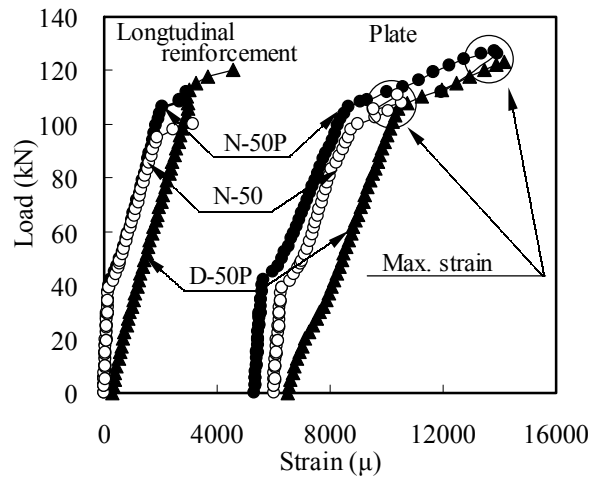


Fig. 11 Relationships between load and strains of longitudinal reinforcement and plate

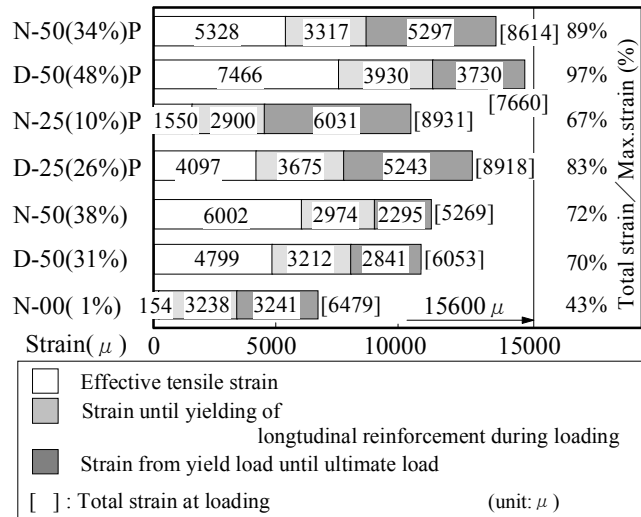


Fig. 12 Plate strain

The relationship between peeling strain and effective tensile strain of the plate is shown in Fig. 13. Plate peeling strain was calculated by decrementing the effective tensile strain from the total plate strain at mid span, since the all specimens failed immediately after peeling of the plate. The plate peeling strain corresponds to an increase in plate strain during loading, as indicated in Fig. 12. In specimens without the intermediate anchoring device, it tends to decrease with increasing effective tensile force. However, the plate peeling strain was greater than 5,000 μ whatever the deteriorated state of the beam was.

In this study, the bonded length of the plate is 930mm. On the other hand, a recent study reported that the plate peeling strain was 4,000-5,000 μ when flexural loading tests were carried out on RC beams strengthened using

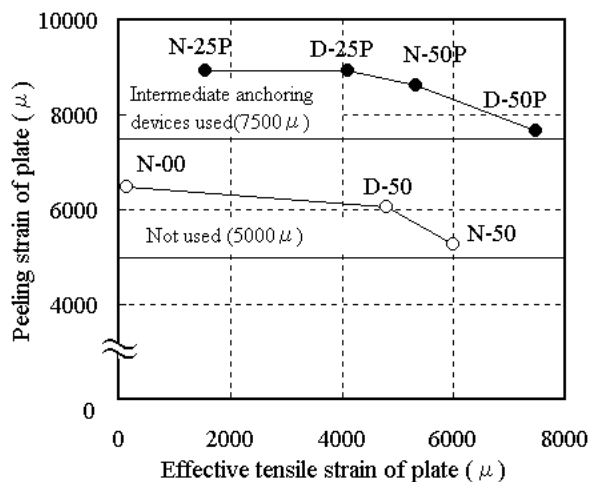


Fig. 13 Relationship between peeling strain and effective strain of plate

non-tensioned CFRP plates (width: 48 mm; thickness: 0.96 mm; bond length: 800 mm) [10]. Generally, it is expected that the peeling strain of a plate will be influenced by plate thickness, concrete strength, surface treatment at the bonding zone, and other factors. However, both this study and the recent study quoted here indicate that peeling strain is approximately  $5,000 \mu$  for a CFRP plate of 50 mm width and 2 mm thickness when bonded over a length of about 900 mm.

Plate peeling strain was always higher when an intermediate anchoring device was used, no matter what the deteriorated state of the beam was. For any effective tensile force this increment in peeling strain was about  $2,500 \mu$ . In these tests, the steel plate comprising the intermediate anchoring device was anchored by simply tightening the bolt as far as possible by hand, and no attempt was made to control this tightening torque, even though it introduces bearing stress at the plate surface. However, it is thought that this tightening torque has no effect on the plate peeling strain, because the increment in peeling strain was about  $2,500 \mu$  in all cases. That is, in strengthened RC beams with intermediate anchoring devices, the plate peeling strain exceeded  $7,500 \mu$  in all cases.

#### d) Load-bearing capacity

The ultimate load of all specimens is shown in **Table 7**. The ultimate load was calculated as the RC beams with single reinforcement, because the amount of compression reinforcement was relatively small. The ultimate load of beams strengthened with tensioned CFRP plates was higher than that of the reference beam with no strengthening, whatever the degree of beam deterioration was. However, the ultimate load was lower than the ultimate load calculated on the assumption that perfect bonding between plate and concrete was obtained. To compensate for this, a simple method calculating the ultimate load was examined. The model provided in “Standard Specifications for Design and Construction of Concrete Structures — Design” (JSCE) [11] was used for the stress-strain curves of concrete and reinforcement. The model for the stress-strain curves of the plate was linear from the origin to the intersection of tensile strength and maximum strain.

As a simple method for calculating the ultimate load of prestressed concrete (PC) structure with an un-bonded tendon or external tendon, the tendon stress is obtained using Equation (1) [5] as given below.

$$f_{ps} = f_{pe} + \Delta f_{ps} \quad (1)$$

where,  $f_{ps}$  is the tensile stress of the tendon at the ultimate load,  $f_{pe}$  is the effective tensile stress, and  $\Delta f_{ps}$  is the increase of tendon stress at loading.

It has been confirmed that the ultimate load of a PC structure with an external tendon can be safely and rationally calculated using this equation, in which  $\Delta f_{ps}$  was evaluated to be applicable [12]. In this study, three methods of obtaining  $\Delta f_{ps}$  are examined as shown in **Table 8**, for use in Equation (1), and a proposal is developed for calculating of the RC beams strengthened with plates.

**Table 8** Calculation methods of ultimate load

Method	$\Delta f_{ps}$ calculation method	Distribution of compressive stress of concrete
A	Proposed equation by Naaman [13] for PC structure with un-bonded tendon	Equivalent stress block (maximum strain of concrete: $3500 \mu$ ) [11]
B	Using peeling strain of plate	Fiber method (using stress-strain curve of concrete)
C		Equivalent stress block (maximum strain of concrete: $3500 \mu$ ) [11]

Calculated as RC beam with single reinforcing rod

All RC beams strengthened with tensioned plates failed in flexure immediately after peeling of the plate. This indicates that the beam acts as a PC structure with an un-bonded tendon in bearing the load for the very short period from peeling to concrete compression failure. In method A,  $\Delta f_{ps}$  is calculated on the assumption that the strengthened RC beam is a PC structure with an un-bonded tendon. Equation (2) proposed by Naaman [13] is adopted for  $\Delta f_{ps}$ . This is the equation adopted in AASHTO [14], and it is confirmed that its application to simply supported PC structures with un-bonded tendons is appropriate in Japan [12]. The bond reduction coefficient ( $\bar{Q}_u$ ) at the ultimate load is calculated using Equation (3) as adopted in ASSHTO. Depth (C) from the compression fiber

of the concrete to the neutral axis is calculated by solving quadric equations for  $C$ , substituting Equations (1)-(3) into Equation (4) for the equilibrium of forces in the section using a rectangular compressive stress distribution for the concrete (equivalent stress block).

$$\Delta f_{ps} = \Omega_u E_p \varepsilon_{cu} \left( \frac{d_p}{C} - 1 \right) \frac{L_1}{L_2} \quad (2)$$

$$\Omega_u = \frac{3.0}{\left( \frac{L}{d_p} \right)} \quad (3)$$

$$A_{ps} f_{ps} + A_s f_{sy} = \alpha \cdot f'_c b_w \cdot 0.8C \quad (4)$$

where,  $\Omega_u$  is the bond reduction coefficient at the ultimate load (Equation (3)),  $E_p$  is the plate modulus of elasticity,  $\varepsilon_{cu}$  is the ultimate concrete compressive strain ( $= 3,500 \mu$ ),  $d_p$  is the effective depth of the plate ( $= 201 \text{ mm}$ ),  $C$  is the depth from the compression fiber of the concrete to the neutral axis,  $L$  is the span,  $L_1$  is the loaded span,  $L_2$  is the length of the tendon,  $A_{ps}$  is the sectional area of the plate,  $A_s$  is the sectional area of the reinforcement,  $f_{ps}$  is the tensile stress of the tendon at the ultimate load,  $f_{sy}$  is the yield strength of the reinforcement,  $f'_c$  is the compressive strength of the concrete,  $\alpha$  is the coefficient of reduction of the compressive stress block of concrete ( $= 0.85$ ),  $b_w$  is the sectional width of beam.

In methods B and C, the ultimate load of the strengthened RC beam is calculated from the peeling strain of the plate. Then  $\Delta f_{ps}$  is calculated using Equation (5). In method B, the ultimate load is calculated by the fiber method on the assumption that the plate strain in the ultimate limit state is equal to the peeling strain of the plate, because compressive failure of the concrete does not occur until after peeling of the plate. With this method, concrete stress is calculated from concrete strain in each element using a concrete stress-strain curve on the assumption that the plane remains within the cross section of beam. The depth from the compression fiber of the concrete to the neutral axis is obtained by iterative calculation until the resultant compressive and tensile forces balance. This method adequately yields the distribution of strain over the cross section at the point of plate peeling. The cross section in the depth direction is divided into eighty fibers.

In the method C, the ultimate load is calculated using equivalent stress blocks on the assumption that the ultimate concrete strain is  $3,500 \mu$ . Where the reinforcement yields at flexural failure, the depth from the compression fiber of the concrete to the neutral axis can be calculated directly. And the ultimate load is simple to calculate in comparison with method A.

$$\Delta f_{ps} = E_p \varepsilon_{peel} / \gamma_p \quad (5)$$

where,  $\varepsilon_{peel}$  is the specified value of plate peeling strain at mid span, which is assumed to be  $7,500 \mu$  and  $5,000 \mu$  for the strengthened beam with and without an intermediate anchoring device respectively, on the basis of **Fig. 13** and  $\gamma_p$  is a material factor for the peeling strain ( $=1.0$ ).

The calculated values of ultimate load and the ratios of experimental values ( $P_{u,exp}$ ) to calculated values ( $P_{u,cal}$ ) are shown in **Table 7** and **Fig. 14**, respectively. Method A calculates  $\Delta f_{ps}$  assuming a PC structure with no bonding between concrete and plate. In this case, the plate strain increase ( $\Delta f_{ps} / E_p$ ) is  $400\text{-}600 \mu$ , only one-tenth that of the plate peeling strain. Consequently, the ultimate load calculated by method A was much smaller than the experimental value. This result demonstrates that effective bonding is achieved between concrete and plate, thus increasing the ultimate load-bearing capacity of the

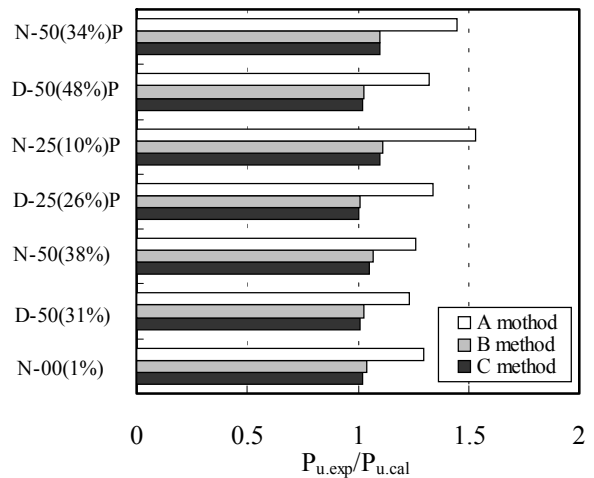


**Fig. 14** Ratio of experimental value ( $P_{u,exp}$ ) to calculated value ( $P_{u,cal}$ )

strengthened beams.

On the other hand, the ratio of experimental value to calculated value in the case of method B ( using the fiber method) is about 1.0, indicating that method B gives an accurate evaluation of the ultimate load of strengthened RC beams. Finally, the ratio of experimental value to calculated value in the case of method C ( using equivalent stress blocks) is also about 1.0. However, strengthened beams failed in flexure immediately after peeling of the plate and before the concrete compressive strain of the beam reached the ultimate strain ( $3,500 \mu$ ). For this reason, it is not considered always appropriate to use the assumption of equivalent stress blocks ( $\epsilon_{ci}$ :  $3,500 \mu$ ). In contrast, the compressive fiber strain at peeling of the plate calculated using method B is  $1,500 \sim 2,600 \mu$ , and it is inferred that the distribution of concrete strain over the cross section at peeling of the plate is evaluated correctly in this case. Considering these results, the proposal is to apply method B for calculations of the ultimate load of strengthened RC beams, since it properly accounts for the distribution of strain over the cross section.

## 5. FATIGUE LOADING TEST OF STRENGTHENED RC BEAMS

### 5.1 Outline of experiment

A summary of the fatigue loading tests is given in **Table 9**. In the Series I tests, live load “B” (245kN) [16] is assumed to act on a road bridge designed for a “TL-20” live load (196kN) [15] , and the effects of tensile force induced in the CFRP plate on the fatigue strength of the strengthened structure were examined. In the Series II tests, the flexural fatigue behavior of beams strengthened with tensioned CFRP plates was examined.

In the Series I tests, a sound RC beam and a deteriorated RC beam were used. The ratio of the tensile force and the tensile strength of the plate were 0 and 50% in sound RC beam and deteriorated RC beam respectively. The deteriorated RC beam was fitted with intermediate anchoring devices.

In the Series II tests, sound RC beams were used. In all beams, the tension applied to the plate was 50% of the plate tensile strength, and intermediate anchoring devices were installed. The upper loading ratios were 70%, 60%, and 50% of the ultimate load. Beams that had not failed at 2 million cycles of loading were statically loaded to estimate the residual ultimate load.

**Table 9** Summary of fatigue loading tests

Series	Specimen	Introduction of crack before strengthening	Strengthening method		Fatigue loading conditions		
			Tension force of plate (kN)	Intermediate anchoring device	Peak load (kN)	Minimum load (kN)	Frequency (Hz)
I	I -N-00	Not introduced	11.4 [5%]	Not used	26.0	11.0 (8.7%)	0.5~3.0
	I -D-50P	Introduced	116.8 [50%]	Used	~85.1*		0.6~4.0
II	II -N-50P-70	Not introduced	116.8 [50%]	Used	88.2 (70%)	11.0 (8.7%)	1.5
	II -N-50P-60				75.6 (60%)		1.0
	II -N-50P-50				63.0 (50%)		0.5

\*: Fatigue loading pattern in series I is shown in **Fig. 15**, [ ] :Tensile force/tensile strength of plate  
 ( ) : Peak load/ultimate load (126kN) of N-50P specimen in static loading test

### 5.2 Loading method

The specimens used for the fatigue loading tests had a span of 2,860 mm and a flexural span of 300 mm, as shown in **Fig. 8**. The fatigue loading pattern used for Series I is shown in **Fig. 15**. The peak and minimum loads were 26.0 kN (live load “B”) and 11.0 kN (dead load), respectively, until 2 million cycles of loading. Thereafter, after each  $20 \times 10^4$  cycles of loading, the peak load was increased, and loading continued until fatigue failure of the beam. Each increment in peak load was 9.8 kN. The peak and minimum loads were determined from longitudinal reinforcement stress in the center span, assuming that live load “B” and the dead load were applied to a non-strengthened original bridge (span:  $5 \times 15 \text{ m} = 75 \text{ m}$ ) designed for a “TL-20” live load. The tensile stress of the longitudinal reinforcement in the center span of the non-strengthened bridge was  $181 \text{ N/mm}^2$  when live load “B” was applied, so the initial peak load was determined by calculating the load at which the tensile stress of the

reference beam without strengthening (specimen N in Table 7) reached 181 N/mm<sup>2</sup>. The tensile stress in the center span was 76.7 N/mm<sup>2</sup> upon loading of the dead load, so the minimum load was also determined in the same way as the initial peak load. In the Series II tests, the peak load ratios were 70%, 60%, and 50% of the ultimate load (D-50P: 126 kN). The minimum load was 11.0kN (8.7%).

Sinusoidal loading was applied using a servopulsator. It was confirmed that the peak load was applied correctly by following the deflection at mid span, and the frequency of fatigue loading was 0.5-4 Hz, as shown in Table 9. A static loading test was carried out during interruptions of the fatigue loading test after every 10-50 x 10<sup>4</sup> cycles.

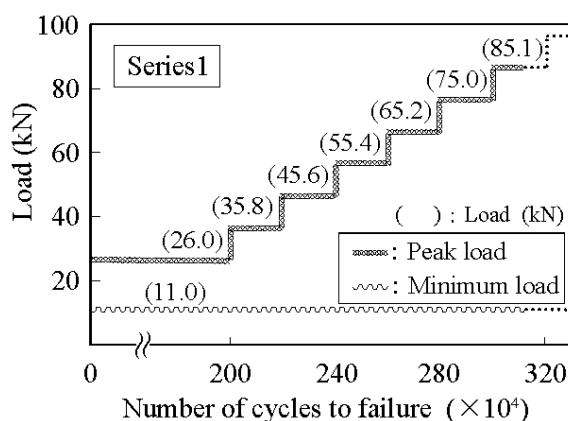


Fig. 15 Fatigue loading pattern for Series I

### 5.3 Test results and discussions

The results of the fatigue loading tests are given in Tables 10 and 11. Within the range of loading frequency used in this study, the effects of frequency on the fatigue behaviors of beam appear relatively small. Therefore, loading frequency is not considered as a parameter in the discussion that follows. In all specimens used for static loading tests except for D-25P and D-50P, it was not possible to introduce the target tension into the plate. For specimens subjected to fatigue loading, the plate was made a little shorter than the design length, and as a result it was possible to introduce the target tension of 50% of plate tensile strength in all cases. Failure of the plate was not observed even

Table 10 Results of Series I fatigue loading tests

Peak load (kN)	I -N-00 (effective tensile force ratio $\eta = 15\%$ )					I -D-50P (effective tensile force ratio $\eta = 50\%$ )				
	Number of cycles $N$	$f_{srd}$ (N/mm <sup>2</sup> )	$N_{sf}$	$N/N_{sf}$	$M$	Number of cycles $N$	$f_{srd}$ (N/mm <sup>2</sup> )	$N_{sf}^{**}$	$N/N_{sf}$	$M$
26.0	2,000,000	84.9	$1.74 \times 10^9$	0.0011	0.0011	2,000,000	(-11 ~ -0.5)	—	—	—
35.8	200,000	138.2	$2.99 \times 10^7$	0.0067	0.0078	200,000	(-11 ~ 7.6)	—	—	—
45.6	200,000	189.4	$2.17 \times 10^6$	0.0922	0.1000	200,000	88.7	$1.27 \times 10^9$	0.0002	0.0002
55.4	200,000	240.0	$3.02 \times 10^5$	0.6623	0.7623	200,000	141.2	$2.66 \times 10^7$	0.0075	0.0077
65.2	200,000	290.7	$6.09 \times 10^4$	3.2841	4.0464	200,000	192.1	$2.04 \times 10^6$	0.0980	0.1057
75.0	92,461	341.4	$1.60 \times 10^4$	5.7788	9.8252	92,461	242.8	$2.91 \times 10^5$	0.3177	0.4234
						107,539			0.3695	0.7929
85.1	—	—	—	—	—	67,024	294.9	$5.74 \times 10^4$	1.1677	1.9606
Total*	2,892,461	$M = \sum (N/N_{sf}) = 9.83$				3,067,024	$M = \sum (N/N_{sf}) = 1.96$			
Failure pattern	Failure of longitudinal reinforcement					Peeling of plate → Failure of longitudinal reinforcement				

\* : Fatigue life (number of accumulated cycles =  $\sum N$ )

\*\* : Fatigue life ( $N_{sf}$ ) was calculated as  $\alpha_p = 0$  ( $\alpha_p$  : stress of reinforcement due to permanent load) by JSCE Equation (7).

Table 11 Results of Series II fatigue loading tests

Specimen	$\eta$ (%)	Peak load (kN)	Ultimate load* (kN)	Peak load ratio (%)	Minimum load ratio (%)	Fatigue life $N$
II -N-50P-70	53	88.2	125.4	70.3	8.8	192,581
II -N-50P-60	51	75.6	124.2	60.9	8.9	647,417
II -N-50P-50**	49	63.0	123.0	51.9	8.9	2,000,000

$\eta$  : Measured tensile force / tensile strength of plate

\* : Ultimate load was calculated using method B in order to consider effective tensile force of plate in each specimen.

\*\* : Static loading test was carried out after 2 million cycles of loading

at fatigue failure of the beam. The end tensioning devices and intermediate anchoring devices remained sound in all tests, as did the concrete around them. No deterioration was observed even at fatigue failure of the beams.

a) Series I

The results of the Series I fatigue loading tests are shown in **Table 10**. Beams strengthened with CFRP plates retained sufficient strength up to 2 million cycles of loading. Specimen I -N-00 failed under fatigue loading when the peak load was 75.0 kN, and total number of cycles to failure was about  $289 \times 10^4$ . The failure mode was fatigue failure of the longitudinal reinforcement. On the contrary, specimen I -D-50P failed under fatigue loading when the peak load was 85.1 kN, and the total number of cycles to failure was about  $307 \times 10^4$ . This is considerably and more than that for specimen I -N-00. The failure mode of specimen I -D-50P was peeling of the plate. The delamination, which showed the peeling of the plate, occurred in the first stage of fatigue failure of specimen I -D-50P. In the next stage, after only several dozen more cycles, final failure occurred due to fatigue failure of the longitudinal reinforcement, since the tensile stress of the reinforcement rose with peeling of the plate.

Generally, the safety of RC beams with respect to flexural fatigue failure under air-dry conditions is examined by investigating the reinforcement under variable loading [17]. Here, the cumulative ratio of loading cycles applied to the reinforcement under variable loading is calculated, and accumulated damage examined. The ratio of cumulative cycles is shown in **Table 10**, as calculated using Equation (6). The reinforcement stress amplitude is calculated using the fiber method on the assumption that the plane remains and using the stress-strain relationship of each material as in Section 4 d). The fatigue life ( $N_{sf}$ ) of the reinforcement under cyclic loading at constant stress amplitude is calculated using Equation (7), as given in the JSCE Specifications [11]. It must be noted, however, that Equation (7) is based on results for partial one side pulse fatigue tests. For the I -D-50P specimen, where the tensile stress of the longitudinal reinforcement at the minimum load becomes compression, the stress amplitude is given by  $\sigma_{sp} = 0$  ( $\sigma_{sp}$  : reinforcement stress induced by the permanent load) [18]. When the ratio of the number of cycles at stress  $i$  is less than 0.0001, the ratio of number of cycles was not accumulated as regardless of the effect of fatigue properties.

$$M = \sum_{i=1}^m \frac{N_i}{N_{sfi}} \quad (6)$$

$$f_{srd} = 190 \frac{10^a}{N^k} \left( 1 - \frac{\sigma_{sp}}{f_{ud}} \right) / \gamma_s \quad (7)$$

where,  $M$  is the ratio of cumulative number of cycles,  $N_i$  is the number of cycles at stress  $i$ ,  $N_{sfi}$  is the fatigue life at stress  $i$  as calculated from the  $S$ - $N$  diagram,  $f_{srd}$  is the calculated value of reinforcement stress amplitude (fatigue strength),  $\sigma_{sp}$  is the reinforcement stress induced by the permanent load,  $f_{ud}$  is the tensile strength of the reinforcement,  $\gamma_s$  is a material factor of reinforcement,  $a = k_o(0.81-0.003 \phi) = 0.762$ ,  $\phi$  is diameter of the reinforcement (= 16 mm),  $k_o$  is a coefficient of surface shape of the reinforcement (= 1.0), and  $k$  is a coefficient (= 0.12).

In the case of specimen I -N-00, the stress amplitude of the reinforcement becomes relatively large because the plate tension is small. As a result, the damage due to cyclic loading begins to accumulate from the beginning of fatigue loading. Consequently, the ratio of cumulative cycles ( $M$ ) was 9.83, and it is thought that fatigue failure of the reinforcement occurred before peeling of the plate. On the contrary, the stress amplitude of the reinforcement in case of specimen I -D-50P is relatively small because the plate tension is high. Therefore, the ratio of cumulative cycles ( $M$ ) was only 0.42 at the point when fatigue failure of the reinforcement occurred in specimen I -N-00 ( $N$  is about  $289 \times 10^4$ ), so almost no damage was accumulated through cyclic loading. As a result, it is thought that the final peak load of specimen I -D-50P was greater than that of specimen I -N-00, and the peeling of the plate happened before fatigue failure of the reinforcement.

The relationship between crack width and number of cycles is shown in **Fig. 16**. Both maximum crack width at the peak load and the residual crack width are shown in the figure. Both increased at 2 million cycles of loading with the initial peak load for specimen I -N-00. By comparison with specimen I -N-00, the crack width of specimen I -D-50P at initial loading ( $N = 1$ ) was larger because, prior to strengthening, loading was applied to specimen I -D-50P until the longitudinal reinforcement yielded. However, the crack was no wider at peak load after 2 million cycles, and the residual crack width remained about 0.015 mm even if the peak load was increased. This confirms

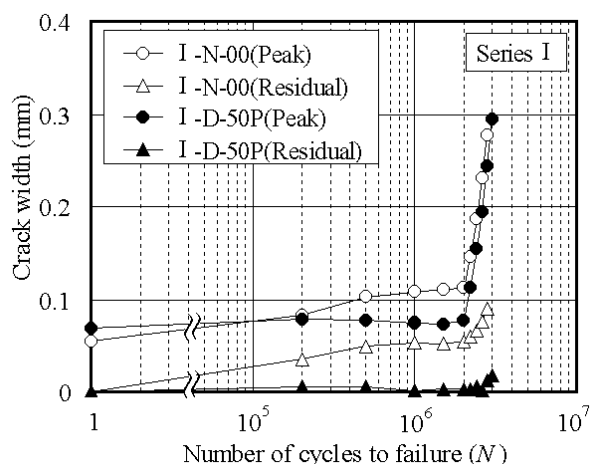


**Fig. 16** Relationship between crack width and number of cycles to failure

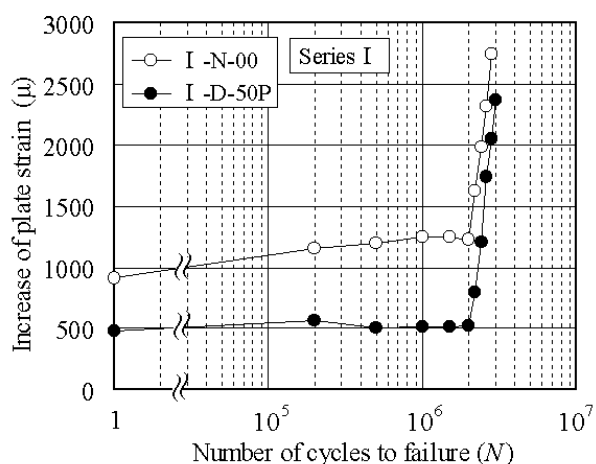


**Fig. 17** Relationship between increase in plate strain and number of cycles to failure

that a higher tension very effectively controls crack.

The relationship between plate strain and the number of cycles is shown in **Fig. 17**. The plate strain in specimen I-N-00 increased during cyclic loading at the initial peak load because the plate tension was low. The rise in plate strain in the case of specimen I-D-50P was smaller up to a peak load of 75.0 kN, because the higher tension very effectively controlled crack width.

#### b) Series II

The results of the Series II fatigue loading tests are shown in **Table 11**. The number of cycles to failure in the case of specimens II-N-50P-70 and II-N-50P-60 was about  $19 \times 10^4$  and  $65 \times 10^4$ , respectively. Both failed when the longitudinal reinforcement failed after peeling of the plate. On the contrary, specimen II-N-50P-50, which was subjected to a comparatively low peak load, did not fail up to 2 million cycles of loading. However, partial peeling of the plate near the flexural crack, which was comparatively wide was observed.

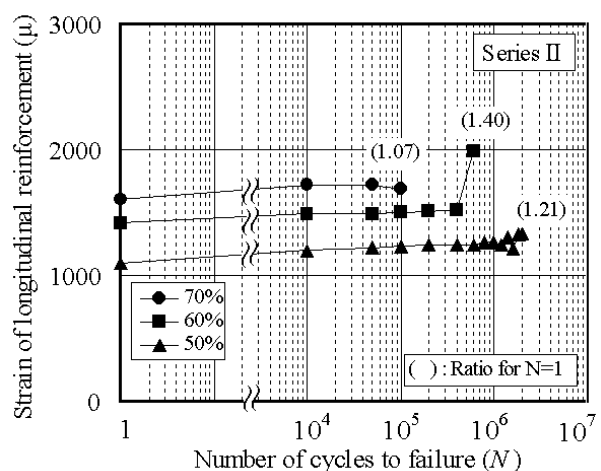


**Fig. 18** Relationship between strain of longitudinal reinforcement at peak load and number of cycles

The relationship between reinforcement strain at the peak load and number of cycles is shown in **Fig. 18**. The ratio between the final measurement of reinforcement strain and that at the initial load ( $N = 1$ ) is also shown. The reinforcement strain of specimen II-N-50P-60 increased suddenly at the final measurement ( $N = 60 \times 10^4$ ). In the case of specimen II-N-50P-50, the reinforcement strain also increased at the 2 million cycles. This is thought to indicate partial peeling of the plate at this time in the case of specimen II-N-50P-60. On the other hand, the increase of plate strain in each specimen was relatively small except for in the final measurement, and behavior was similar to the relationship between reinforcement strain and number of cycles when the normal RC beam failed through fatigue of the reinforcement in the flexural fatigue test. This result was obtained because the bond between plate and concrete was sound. The reinforcement strain in RC beam strengthened with a tensioned CFRP plate can be estimated accurately by the fiber method until peeling of the plate.

The  $S-N$  diagram and regression equation for the Series II tests are shown in **Fig. 19**. Here,  $S_r$  is the ratio of load amplitude to ultimate load,  $S_{max}$  is the ratio of peak load to ultimate load, and  $S_{min}$  is the ratio of minimum load to ultimate load. The ultimate load was calculated using method B as described in Section 4 in consideration of the effective tension force on each plate. The  $S-N$  curve for the longitudinal reinforcement is also shown in **Fig. 19**. This

was calculated by the least squares method using the  $S_r$  value for each specimen and the fatigue life of the reinforcement, as calculated by the same method as used for Series I. The failure mode of specimens II-N-50P-70 and II-N-50P-60 was peeling of the plate, while some peeling occurred in specimen II-N-50P-50 after 2 million cycles of loading. Based on these results, the regression equation for the  $S-N$  diagram was calculated by the least squares method on the assumption that the failure mode of all beams was peeling of the plate (marked by ●). This yields good correlation between the regression equation and the experimental values, indicating that the peeling fatigue strength of the plate can be accurately calculated using the regression equation. The fatigue strength at 2 million cycles of RC beams strengthened with tensioned CFRP plates was 51% ( $S_{min}=8.9\%$ ) of the ultimate load, and the failure mode was peeling of the plate. In similar fatigue loading tests on RC beams (compressive strength of concrete: about 55 N/mm<sup>2</sup>; tensile reinforcement ratio: 2.8%) using reinforcement with similar tensile strength as in this study, it was clarified that the fatigue strength after 2 million cycles of beams that failed through fatigue of the reinforcement in air-dry conditions was 60% of the ultimate load [19]. The fatigue strength at 2 million cycles of beams strengthened with tensioned CFRP plates was smaller than in this result.

Where  $S_r$  is greater than 0.45, the fatigue life of the longitudinal reinforcement is lower than in RC beams strengthened with tensioned CFRP plates. This is because Equation (7) provides safety in the fatigue life of the reinforcement [20]. In the Series I tests, two failure modes were observed: failure of the reinforcement and peeling of the plate. It is, therefore, necessary to evaluate the flexural fatigue limit state in the actual design of RC beams strengthened with tensioned CFRP plates, based on both the fatigue strength of the reinforcement [17] and the peeling fatigue strength of the plate.

c) Residual ultimate load in Series II

Specimen II-N-50P-50, which did not fail even after 2 million cycles of loading, was statically loaded to estimate its residual ultimate load capacity. The results of this residual static loading test and the relationship between load and deflection at mid span are shown in Table 12 and Fig. 20, respectively. The relationship between load and deflection of specimen D-50P in the static loading test is also shown in Fig. 20. Local peeling of the plate occurred during the fatigue loading did not develop under static loading. Specimen II-N-50P-50 failed in flexure immediately after peeling of the plate.

The deflection of specimen II-N-50P-50 only exceeded that of specimen D-50P by about 2 mm at the peak load level of the fatigue loading test (63.0 kN). However, this deflection increased at the ultimate load, and the residual ultimate load capacity of specimen II-N-50P-50 was 114 kN, which is smaller than that of specimen D-50P (126kN). The cause of this was deterioration of the bond between concrete and plate after 2 million cycles of loading at the peak load (peak load ratio: 50%) corresponding to fatigue strength after 2 million cycles (peak load ratio: 51%) of the RC beam strengthened with a

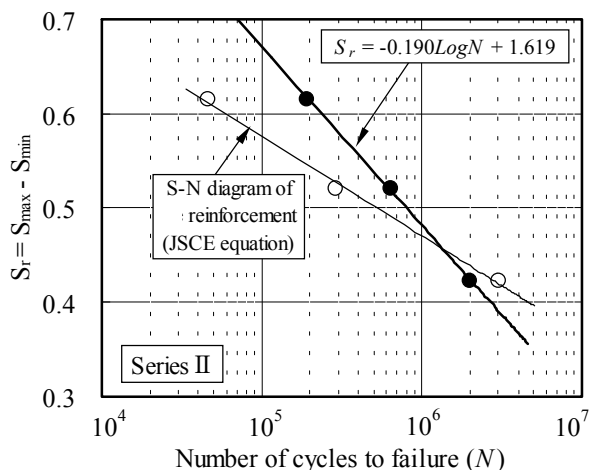


Fig. 19 S - N diagram for Series II

Table 12 Results of residual static loading tests (II-N-50P-50)

Peeling strain of plate ( $\mu$ )	Ultimate load (kN)		
	Experimental value ①	Calculated value* ②	①/②
7,170	114	121	0.94

\* : Method B ( $\epsilon_{peel}=7,170 \mu$ )

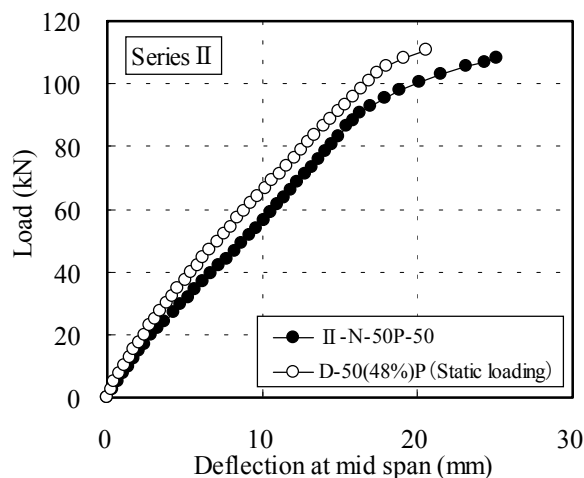


Fig. 20 Relationship between load and deflection at mid span (II-N-50P-50)

tensioned CFRP plate. Consequently, the peeling strain of the plate was  $7,170 \mu$ , which is less than that of specimen D-50P ( $7,660 \mu$ ) and the specified peeling strain ( $\varepsilon_{peel} = 7,500 \mu$ ) assumed in Equation (5). So the ultimate load was calculated by method B which the peeling strain of the plate was  $7,170 \mu$ . The resulting ratio of experimental value to calculated value is 0.94. This means that the residual ultimate load capacity of strengthened RC beams can approximately be evaluated from the peeling strain of the plate in static loading after a fatigue loading test using method B. In the next stage of this study, it will be necessary to examine the fatigue bonding properties of the plate and concrete, allowing the characteristic value of fatigue resistance to peeling of the plate to be determined.

## **6. CONCLUSIONS**

The aim of this study is to encourage practical applications of a method of strengthening concrete structures using tensioned carbon fiber reinforced polymer plates (CFRP plates). The static loading tests and fatigue loading tests of RC beams strengthened with such plates were carried out, and the strengthening effects were examined. The following results can be drawn from the investigation:

- (1) If the CFRP plate (width: 50 mm; depth: 2 mm) is anchored by embedding it for a length of more than 250 mm, the tensile failure mode is failure of the plate. With such an anchorage, it is thought full advantage can be taken of the high strength of CFRP. The tensile strength of the CFRP plate as calculated by  $3\sigma$  method using the results of tensile tests was 234 kN.
- (2) Flexural failure of beams strengthened with tensioned CFRP plates occurred immediately after the peeling of the plate. However, the ultimate load of the strengthened beams was high as compared with that of a reference beam without strengthening, and the strengthening effect improves as the tension force on the plate is increased.
- (3) Peeling of the CFRP plate is influenced largely by the use of intermediate anchoring devices. With this strengthening method, the strengthening effect was improved by increasing the effective tension force on the plate through use of an intermediate anchoring device.
- (4) The peeling strain of the plate at mid span was found to be  $7,500 \mu$  and  $5,000 \mu$  for beams with and without intermediate anchoring devices, respectively. The ultimate load of RC beams strengthened with tensioned CFRP plates can be evaluated appropriately from this peeling strain using the fiber method (method B).
- (5) In fatigue tests under the same loading conditions, the fatigue life of RC beams strengthened with CFRP plates tensioned to 50% of the plate tensile strength was greater than when the plates were tensioned with 15% of the strength. However, by strengthening RC beams designed for “TL-20” live loads with tensioned CFRP plates, adequate fatigue strength was achieved up to 2 million cycles of loading regardless of the tension force applied to the plate if the initial peak load corresponded to the “B” live load.
- (6) The fatigue strength of RC beams strengthened by tensioned CFRP plates after 2 million cycles was about 50% of the ultimate load, and the failure mode was the peeling of the plate.
- (7) The residual ultimate load capacity of an RC beam strengthened with a tensioned CFRP plate after 2 million cycles of loading to a peak load corresponding to its fatigue strength at 2 million cycles was smaller than the ultimate load of a similar strengthened beam under static loading. The residual ultimate load capacity of strengthened RC beams can be approximately evaluated using method B based on the peeling strain of the plate at static loading after a fatigue loading test.

## **References**

- [1] Japan Society of Civil Engineers: Standard Specification for Design and Construction of Concrete Structures (Maintenance), 2001 (in Japanese)
- [2] Public Works Research Institute, Bridge Laboratory, Bridge Structure Team, Technical Workshop on Methods of Repair and Strengthening: Joint Research Report (III) on Repair and Strengthening of Concrete Members— Design and Construction Concept for Repair and Strengthening of Bridge Concrete Members by Method with Externally Bonded Carbon Fiber Sheets—, 1999
- [3] Japan Society of Civil Engineers: Repair and Strengthening Concept for Concrete Structures Using Continuous

Fiber Sheet, Concrete Library 101, pp.21-23, 2000

[4] Japan Prestressed Concrete Contractors Association: Recommendation for Strengthening Manual of Concrete Bridges by External Tendon Method, pp.75-91, Oct. 1998

[5] Japan Society of Civil Engineers: Recommendation for Strengthening Concept for Concrete Structures, Concrete Library 95, 1999

[6] Mashima, M., Kosa, K., and Ohno, S: Fiber Reinforced Cement/Concrete Composite Materials, Gihodo Shuppan, pp.45-50, 1994

[7] Harada, T., Idemitsu, T., Khin, M., Fukuda, K., and Watanabe, A.: A Study on Anchorage Method for Continuous Fiber Reinforcing Materials (FRP) Using Highly Expansive Material, Proceedings of the Japan Society of Civil Engineers, No.627/V - 44, pp.77-90, 1999

[8] Sekishima, K., Kogure, A., Suzuki, H., and Ohtsuka, Y.: Study on Retrofitting Method with Fiber Reinforced Plastics Plate as Prestressing Tendon, Proceedings of JCI Symposium on Repair and Cathodic Protection of Concrete Structures, Japan Concrete Institute, pp.85-92, 1994

[9] Wu, Z. S., Matsuzaki, T., Fukuzawa, K., and Kanda, K.: Strengthening Effects on RC Beams of Externally Prestressed Carbon Fiber Sheets, Proceedings of the Japan Society of Civil Engineers, No.641/V - 46, pp.153-165, 2002

[10] Kohzo, K., Kobatake, Y., Hirata, R., and Tsuchiya, Y.: Flexural Strengthening of Existing RC Beams with CFRP Plates, Proceedings of 40th Conference of Material Association, Science Council of Japan, pp.216-217, 1996

[11] Japan Society of Civil Engineers: Standard Specification for Design and Construction of Concrete Structures (Design), pp.17-44, 1996

[12] Kosaka, H., Kawada, N., and Tsuno, K.: A Study on the Ultimate Bending Behavior of Prestressed-Concrete Bridges Using External Tendons, Proceedings of the Japan Society of Civil Engineers, No.613/V -42, pp.147-164, 1999

[13] Naaman, A. E., and Alkhairi, F.M.: Stress at Ultimate State in Unbonded Post-Tensioning Tendons: Part 2 – Proposed Methodology, ACI Structural Journal, Vol.88, No.6, pp.683-692, Nov.-Dec. 1991

[14] AASHTO LRFD Bridge Design Specifications, SI Units First Edition, 1994

[15] Japan Road Association: Design Specifications for Highway Bridges, Part Concrete bridge, 1978

[16] Japan Road Association: Design Specifications for Highway Bridges, Part Concrete bridge, 1996

[17] Matsushita, H., and Takakura, K.: Characteristic Strength of Concrete and Resistant Design Shear Force in Fatigue for the Limit State Design Method, Concrete Journal, Vol.22, No.8, pp.14-23, Aug. 1984

[18] Railway Technical Research Institute: Design Standard for Railway Structures—Concrete Structures, Maruzen, pp.69-77, 1984

[19] Nishibayashi, S., Inoue, S., Yoshino, A., and Kumano, T.: Prediction of Fatigue Life of Reinforced Concrete Beam in Water, Proceedings of the Japan Concrete Institute, Vol.12, No.2, pp.287-292, 1990

[20] Okamura, H., and Niwa, J.: Fatigue of Reinforced Concrete Members, Concrete Journal, Vol.21, No.1, pp.22-30, Jan. 1983